

Characterization of Arbitrary Femtosecond Pulses Using Frequency-Resolved Optical Gating

Daniel J. Kane and Rick Trebino

Abstract—We introduce a new technique, which we call frequency-resolved optical gating (FROG), for characterizing and displaying arbitrary femtosecond pulses. The method is simple, general, broad-band, and does not require a reference pulse. Using virtually any instantaneous nonlinear-optical effect, FROG involves measuring the spectrum of the signal pulse as a function of the delay between two input pulses. The resulting trace of intensity versus frequency and delay is related to the pulse's spectrogram, a visually intuitive transform containing both time and frequency information. We prove, using phase retrieval concepts, that the FROG trace yields the full intensity $I(t)$ and phase $\varphi(t)$ of an arbitrary ultrashort pulse with no physically significant ambiguities. We argue, in analogy with acoustics problems, that the FROG trace is in many ways as useful a representation of the pulse as the field itself. FROG appears to have temporal resolution limited only by the response of the nonlinear medium. We demonstrate the method using self-diffraction via the electronic Kerr effect in BK-7 glass and few μJ , 620 nm, linearly chirped, ~ 200 fs pulses.

INTRODUCTION

THE technology of ultrashort pulse measurement has been under development since the advent of ultrashort pulse lasers over two decades ago. Early methods yielded only the intensity autocorrelation of the pulse [1]–[3]. Later developments have achieved the indirect determination of various phase distortions common to ultrashort pulses [4]–[6]. Unfortunately, these methods yield only partial information. Some work has been done to extract the time-dependent intensity $I(t)$ and phase $\varphi(t)$ [or, essentially equivalent to the phase, the instantaneous frequency $\omega(t)$], from these traces using iterative algorithms [7]–[9]. Fundamental inherent ambiguities, including the direction of time, however, remain [8]. It is therefore not possible to determine, for example, the sign of a chirp, unless a second measurement is made after pulse propagation through a known dispersive medium [7], [10]. Other methods yield only $I(t)$ [11], [12] or require a streak camera, [13], [14] and hence lack sufficient temporal resolution. Still other methods have been developed to measure the phase $\varphi(t)$ but are complex, require a reference

pulse, and/or do not yield the intensity [15]–[20]. In an important recent development, however, Chilla and Martinez [21]–[23] have demonstrated a method that directly obtains the pulse shape and phase in the frequency domain. Extending work first performed by Fork *et al.*, [16], [17] their method involves frequency filtering the pulse and cross correlating the filtered pulse with the shorter unfiltered pulse, yielding the group delay versus frequency, which is integrated to yield the phase versus frequency. This result, in conjunction with the spectrum, is the pulse field in the frequency domain, and Fourier transformation then yields the intensity and phase in the time domain without significant ambiguity. This method represents an important development, and it has been successfully used to make measurements of ultrashort pulses [24]. Unfortunately, it is complex and time consuming to perform and is unlikely to achieve single-shot operation. It also requires that the pulse group delay be well defined.

In this paper, we propose and demonstrate an experimentally simpler method, which we call *frequency-resolved optical gating* (FROG), which, in principle, also determines the intensity and phase of a pulse without significant ambiguity. Whereas Chilla and Martinez measured the cross correlation of a particular frequency component of an ultrashort pulse, FROG involves measuring the *spectrogram* of a particular *temporal component* of the pulse (see Fig. 1). FROG does this by spectrally resolving the signal pulse in virtually any autocorrelation-type experiment performed in an instantaneously responding nonlinear medium. The resulting trace of intensity versus frequency and delay is related to a well-known quantity, the spectrogram [25] of the pulse:

$$S_E(\omega, \tau) = \left| \int_{-\infty}^{\infty} E(t)g(t - \tau) \exp(-i\omega t) dt \right|^2 \quad (1)$$

where $g(t - \tau)$ is a variable-delay gate pulse, and the subscript E on S_E indicates the spectrogram's dependence on the pulse field $E(t)$. The gate pulse $g(t)$ is usually somewhat shorter in length than the pulse to be measured, but *not* infinitely short. This is an important point: an infinitely short gate pulse yields only the intensity $I(t)$ and conversely, a CW gate yields only the spectrum $I(\omega)$. On the other hand, a finite-length gate pulse yields the spectrogram of all of the finite pulse segments with duration equal to that of the gate. While the phase information remains lacking in each of these short-time spectra, this loss is

Manuscript received February 14, 1992; revised July 30, 1992. The work of D. Kane was supported by Los Alamos National Labs. The work of R. Trebino was supported by the U.S. Department of Energy, Office of Basic Energy Sciences, Chemical Sciences Division.

D. J. Kane is with Southwest Sciences, Inc., Santa Fe, NM 87501.

R. Trebino is with Combustion Research Facility, Sandia National Laboratories, Livermore, CA 94551.

IEEE Log Number 9205921.

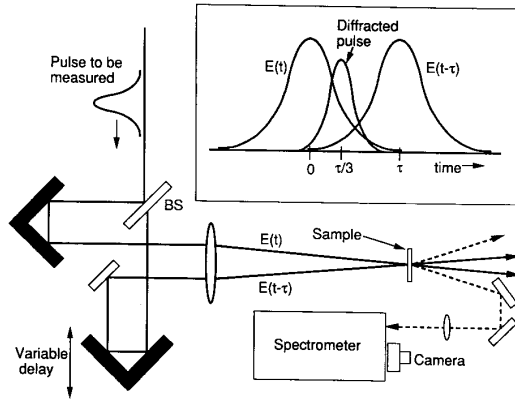


Fig. 1. Experimental apparatus for FROG. FROG involves splitting the pulse and overlapping the two resulting pulses in an instantaneously responding $\chi^{(3)}$ medium. In this paper, we use self-diffraction due to the electronic Kerr effect in glass as the nonlinear-optical process. The diffracted light is then spectrally resolved, and the diffracted intensity measured versus wavelength and delay τ . The resulting trace of intensity versus delay and frequency is related to the spectrogram, a time- and frequency-resolved transform that intuitively displays time-dependent spectral information of a waveform. Inset: Because most of the diffracted light emanates from the times $\tau/3$ of one pulse and $-2\tau/3$ of the other pulse, the diffracted pulse, when spectrally analyzed, indicates the frequencies of these regions of the pulse.

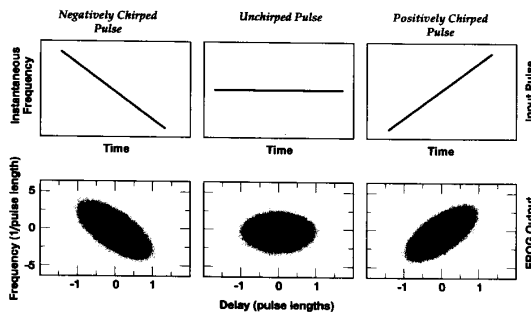


Fig. 2. Spectrograms for negatively chirped, unchirped, and positively chirped Gaussian pulses. Above each are shown the instantaneous frequency versus delay curves for the pulses. A Gaussian window function of width approximately 70% of the pulsewidth was used. These traces are also theoretical self-diffraction FROG traces for negatively chirped, unchirped, and positively chirped Gaussian pulses. The only difference between the spectrogram and FROG traces for the pulses shown here is that the appropriate vertical scale of the instantaneous frequency plots is larger for the spectrograms than for the FROG traces. In other words, the self-diffraction FROG trace amplifies linear chirp somewhat compared to the spectrogram. See Appendix C for further discussion of this effect. (The use of polarization-spectroscopy optical gating for the nonlinear effect in FROG would yield a FROG trace equal to the spectrogram.)

compensated by having the spectrum of an infinitely large set of pulse segments. The spectrogram has been shown to nearly uniquely determine both the intensity $I(t)$ and phase $\varphi(t)$ of the pulse, even if the gate pulse is longer than the pulse to be measured [26], [27] (although if the gate is too long, sensitivity to noise and other practical problems arise [28]). The spectrogram is commonly used in acoustics to visually display a sound wave [25]. It is a natural and intuitive measure, showing the short-time spectrum of the waveform as a function of time. An ex-

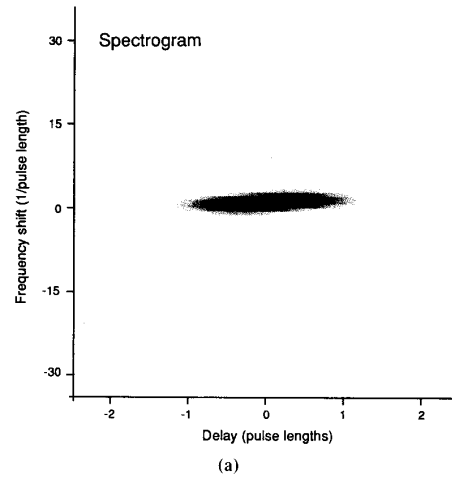
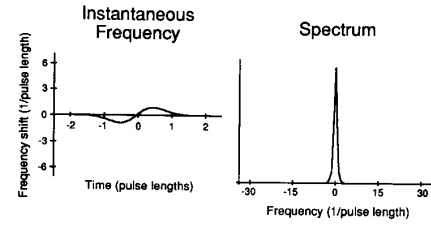


Fig. 3. Theoretical instantaneous frequency versus time, spectrum, spectrogram, and FROG trace for a weakly self-phase-modulated pulse ($Q = 1$). Note that the spectrogram and FROG trace both visually display the pulse instantaneous frequency versus time (see Appendix C). (The use of polarization-spectroscopy optical gating for the nonlinear effect in FROG would yield a FROG trace equal to the spectrogram.)

ample of the spectrogram in everyday life is a musical score. Figs. 2 through 4 give examples of theoretical spectrograms for commonly encountered ultrashort pulses.

In FROG, using self-diffraction as the nonlinear effect, the signal pulse is given by:

$$E_{\text{sig}}(t, \tau) \propto [E(t)]^2 E^*(t - \tau) \quad (2)$$

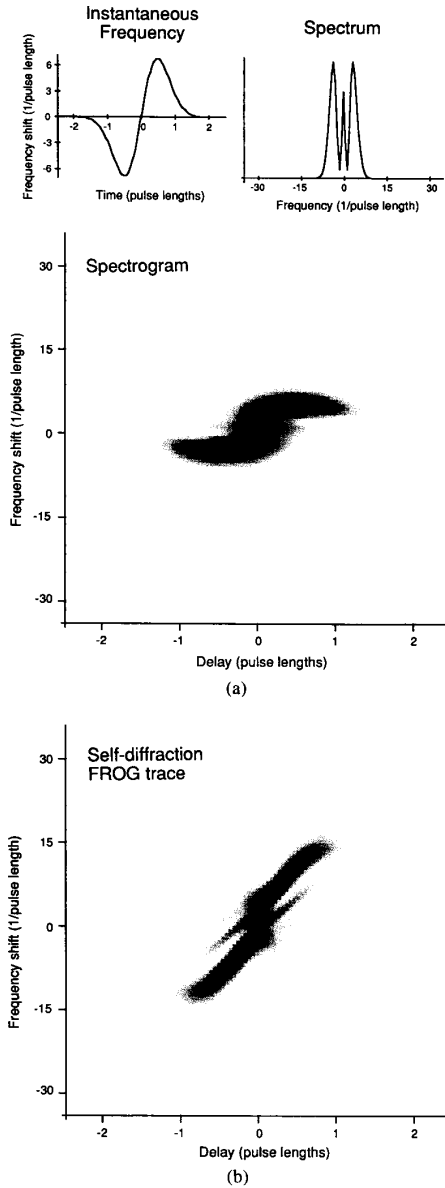


Fig. 4. Theoretical instantaneous frequency versus time, spectrum, spectrogram, and FROG trace for a strongly self-phase-modulated pulse ($Q = 8$). Note that the mean frequency versus delay of both the spectrogram and FROG trace indicates the pulse instantaneous frequency vs. time (see Appendix C). The structure in the both traces indicates the breakup of the spectrum due to self-phase modulation. The additional structure in the FROG trace is a result of the dependence of the FROG trace on the pulse phase at two different times $\tau/3$ and $-2\tau/3$. (The use of polarization-spectroscopy optical gating for the nonlinear effect in FROG would yield a FROG trace equal to the spectrogram.)

so the measured signal intensity $I_{\text{FROG}}(\omega, \tau)$, after the spectrometer is:

$$I_{\text{FROG}}(\omega, \tau) = \left| \int_{-\infty}^{\infty} [E(t)]^2 E^*(t - \tau) \exp(-i\omega t) dt \right|^2. \quad (3)$$

We see that the FROG trace (see Figs. 2 through 4) is thus a spectrogram of the pulse squared $E^2(t)$ although the gate pulse $E^*(t - \tau)$ is a function of the pulse itself. Or, with a change of variables, we can regard $E^*(t)$ as the pulse to be measured, and $E^2(t - \tau')$ as the gate ($\tau' = -\tau$). While algorithms previously developed for determining a waveform from its spectrogram generally require knowledge of the gate function [26], we will show that this is not essential.

To see that the FROG trace essentially uniquely determines $E(t)$ for an arbitrary pulse, it is first necessary to observe that $E(t)$ is easily obtained from $E_{\text{sig}}(t, \tau)$. This is shown in Appendix A. Then it is simply necessary to write (3) in terms of $E_{\text{sig}}(t, \Omega)$, the Fourier transform of the signal field $E_{\text{sig}}(t, \tau)$ with respect to the delay variable τ . We then have what appears to be a more complex expression, but one that will give us better insight into the problem:

$$I_{\text{FROG}}(\omega, \tau) = \left| \int_{-\infty}^{\infty} E_{\text{sig}}(t, \Omega) \cdot \exp(-i\omega t - i\Omega\tau) dt d\Omega \right|^2. \quad (4)$$

Equation (4) indicates that the problem of inverting the FROG trace $I_{\text{FROG}}(\omega, \tau)$ to find the desired quantity $E_{\text{sig}}(t, \Omega)$ is that of inverting the squared magnitude of the two-dimensional (2-D) Fourier transform of $E_{\text{sig}}(t, \Omega)$. This problem, which is called the *2-D phase-retrieval problem*, is well known in many fields, especially in astronomy, where the squared magnitude of the Fourier transform of a 2-D image is often measured [29], [30]. At first glance, this problem appears unsolvable; after all, much information is lost when the magnitude is taken. Worse, it is well known that the 1-D phase retrieval problem is unsolvable [for example, infinitely many pulse fields give rise to the same spectrum, $|\int E(t) \exp(-i\omega t) dt|^2$]. Intuition fails badly in this case, however; two- and higher-dimensional phase retrieval essentially *always yields unique results* [29]–[34]. Only a set of traces of measure zero yields nontrivial ambiguities, and their occurrence, even in the presence of noise, is an event with zero probability. Otherwise, only trivial, unimportant ambiguities (such as a constant phase factor) remain in these problems (see Appendix B). Interestingly, our inability to solve 1-D phase-retrieval problems follows from the *existence* of the Fundamental Theorem of Algebra for polynomials in one variable. Conversely, our ability to solve two- and higher-dimensional phase-retrieval problems follows from the *nonexistence* of the Fundamental Theorem of Algebra for polynomials of two or more variables [29]. The phase-retrieval literature contains additional details regarding these interesting results, including a wide range of algorithms for finding the solutions to these problems, and the interested reader is referred to this literature [29], [35]–[38].

Thus, in principle, the FROG trace uniquely determines the pulse field $E(t)$ for an arbitrary ultrashort pulse.

We will provide in a future publication an iterative algorithm for obtaining the precise pulse field, given a FROG trace (which involves a few variations on currently available methods). Here, instead, we simply curve-fit the experimental FROG trace to a reasonably general model.

More importantly, we would like to point out here that the FROG trace is itself a very convenient representation of the pulse. In acoustics problems, for example, analogous time- and frequency-resolved traces [28] (the spectrogram, Gabor transform, Wigner transform, wavelet transform, etc.) are usually *preferred* to the precise measurements of the pressure wave versus time from which they are calculated [39]. We argue here that the same is true for ultrashort pulses. For reasonably well-behaved pulses, the FROG trace graphically displays the instantaneous frequency as a function of time, subject to a simple correction formula (see Appendix C). In addition, the approximate pulse width is indicated by the extent of the trace along the delay co-ordinate. And, because the FROG trace provides both time and frequency information simultaneously, a plot using the correct scaling yields approximately circular contours of constant intensity for a transform-limited pulse.

FROG has additional advantages: it is inexpensive, simple to implement, and very broadband, appearing very well suited to the measurement of UV pulses. The self-diffraction geometry has negligible phase mismatch, and it is possible to use the polarization-spectroscopy optical-gate geometry, which is automatically phase matched. FROG is readily extendable to a single-shot device, in which the pulse shape and phase may be determined simply by crossing two cylindrical-lens-focused line-shaped beams at an angle, allowing the signal light to pass through a spectrometer, and detecting with a 2-D array detector. One very important feature of FROG is that spectral dispersion occurs after, rather than before (as in the method of Chilla and Martinez), the nonlinear medium, allowing much higher intensity in the nonlinear medium and a simpler alignment. This also avoids the need for frequency scanning, which means that the time required to perform the measurement is proportional to N , rather than N^2 , where N is the number of temporal points desired.

We should point out that the notion of making measurements with both finite time and frequency resolution is certainly not new in the field of ultrafast spectroscopy. It is quite common to measure the spectrum versus delay in excite-probe experiments [40], [41]. Such measurements have been referred to as time-resolved spectral measurements, as well as "spectrochronograms" [42]. We believe, however, that this paper is the first to use these concepts to measure an ultrashort pulse.

In order to demonstrate this method experimentally, we performed a multishot experiment involving amplified fsec pulses. A Rhodamine-6G colliding-pulse mode-locked laser produced < 100 fs pulses at a repetition rate of ~ 100 MHz, and a 10 Hz Nd:YAG-pumped four-stage dye amplifier amplified these pulses to an energy of ~ 200 μ J.

Dispersion compensation using four SF-10 prisms could compress the resulting ~ 200 fs pulses to ~ 100 fs, but such compensation was not used in this experiment. A beam splitter and a neutral-density filter yielded two replicas of the pulse of about 6 μ J each. A high-quality translation stage, with a resolution of 1 μ m, produced variable delay for one pulse train, and a ~ 1 m focal-length lens focused and crossed the two beams at an angle of about 0.5° . The electronic Kerr effect in a 3 mm thick BK-7 window placed at the focus of these two beams provided self-diffraction with $\sim 10^{-4}$ efficiency. The peak intensity at the BK-7 was approximately 25 GW/cm² (an intensity for which we verified an approximately cubic dependence of diffracted energy versus input energy). In addition, we observed negligible spectral broadening or small-scale self-focusing due to the medium. We calculate that the effects of group-velocity dispersion due to the optics and sample medium were negligible at ~ 620 nm. The diffracted beam was attenuated (ND 1.0) and focused onto the 50 μ m slits of a 1/4 m Jarrel Ash spectrometer. A liquid-nitrogen-cooled Photometrics charge-coupled-device (CCD) camera collected the dispersed diffracted light, averaged over 20 shots. (We should point out that signal strengths were sufficient that a thermoelectrically cooled CCD camera would have sufficed and should suffice in most experiments.) The diffracted intensity vs. wavelength was then recorded with a MacIntosh IICI microcomputer.

Diffracted-pulse spectra were obtained for eleven different delays at 67 fs intervals using the unrecompressed, positively chirped ~ 200 fs pulses. These spectra easily revealed a large wavelength chirp over the range of delays used. Fig. 5 shows a density plot of the measured diffracted pulse energy versus wavelength and delay. Because a fast Fourier transform routine is necessarily involved in the analysis of the data, it is important that the delay increment $\delta\tau$ and frequency increment $\delta\nu$ be related by the appropriate relation $\delta\nu = 1/(N\delta\tau)$, where N is the number of delays or frequencies. It was thus necessary to massage the data somewhat. Specifically, spectral data were eliminated, and delay data had to be interpolated. In this manner, an 11×516 array was transformed to a 33×33 array.

We curve-fit the data to a model that allows for double-pulsing and, to some extent, asymmetrical pulses:

$$E(t) = A(t) \exp [i\varphi(t)] \quad (5)$$

where

$$A(t) = \exp \{-a[t/\tau_{\text{ref}}]^2\} + b \exp \{-c[t/\tau_{\text{ref}} - d]^2\} \quad (6)$$

and

$$\varphi(t) = \alpha(t/\tau_{\text{ref}}) + \beta(t/\tau_{\text{ref}})^2 + \gamma(t/\tau_{\text{ref}})^3 + \delta(t/\tau_{\text{ref}})^4 + \epsilon(t/\tau_{\text{ref}})^5 \quad (7)$$

Using the value $\tau_{\text{ref}} = 76$ fs, we obtained a fit with $a = 0.133$, $b = 0.41$, $c = 1.60$, $d = -1.18$, $\alpha = -0.058$, β

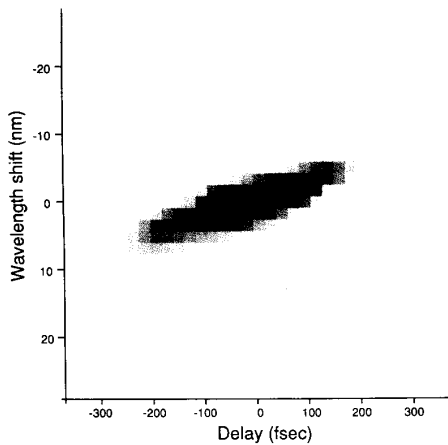


Fig. 5. Experimentally obtained self-diffraction-FROG trace for a ~ 200 fs pulse immediately after amplification. This trace indicates approximately linear positive chirp, as expected.

$= -0.271$, $\gamma = -0.00044$, $\delta = -0.0007$, and $\epsilon = -0.00003$. The FROG trace of the highly asymmetrical derived-pulse is shown in Fig. 6. In view of the uniqueness result relating the FROG trace to the pulse field, the accuracy of the derived field should be indicated by agreement of the measured and derived-pulse FROG traces. We see that the two traces agree reasonably well, indicating reasonably good convergence. To further evaluate the fit, we computed the rms error between the two traces, obtaining 1.9% of peak per point for the 33×33 array, which is better than the noise during the pulse, but worse in the dark regions, and which is reasonable, given the noise in the data. Fig. 7 shows the residuals, which appear random, but small discrepancies exist near the pulse peak, indicating inadequacies in the assumed model. Fig. 8 shows the derived intensity and phase obtained in the fit. Because the phase is approximately an upside-down parabola, the chirp is approximately linear and positive ($\omega(t) = -d\phi/dt$). The main deviation from a simple parabola in Fig. 8 is a linear term, which reflected only a frequency shift from that chosen for the reference pulse frequency in the fit. The derived positively linearly chirped, asymmetrical pulse of about 200 fs in duration agrees with our expectations for an unrecompressed pulse directly from the amplifier.

In order to verify that the pulse intensity obtained using FROG is accurate, we measured the pulse third-order intensity autocorrelation $[\int I^2(t)I(t - \tau) dt]$ by integrating the FROG trace over all frequencies for each delay. Fig. 9 shows the computed third-order intensity autocorrelation of the derived pulse, in good agreement with the experimentally obtained result. This agreement is significant because the chirp is responsible for an increase by a factor of ~ 2 in the pulse length.

To partially check the accuracy of the derived phase, we have also independently measured the spectrum of the pulse. For comparison, we have computed the spectrum of the derived pulse by Fourier transforming the derived

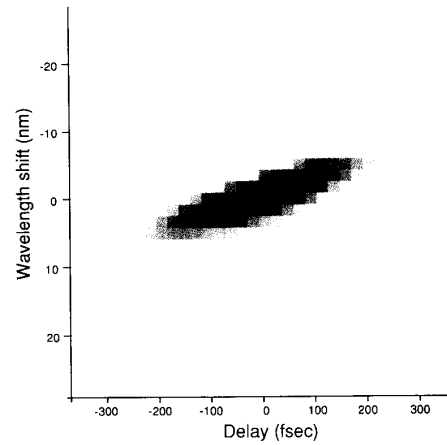


Fig. 6. The FROG trace of the derived pulse for the data in Fig. 5.

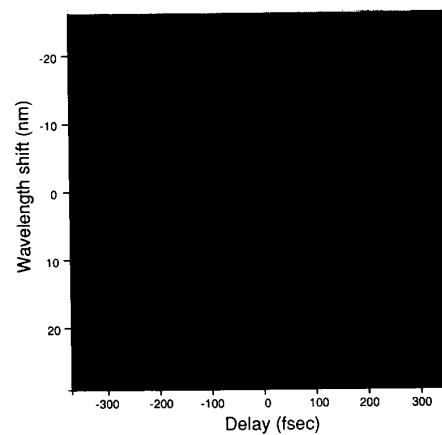


Fig. 7. The residuals of the fit. This figure is the difference between Figs. 6 and 5, with each plot normalized to have unity maximum. The scale here is from -1 (black) to 1 (white). Observe that the residuals are mainly gray and deviations are relatively random, indicating a reasonably good fit.

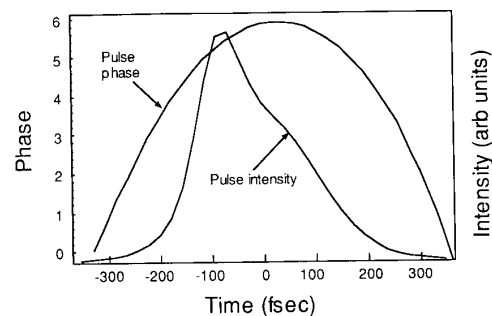


Fig. 8. The derived intensity and phase for the experimentally measured pulse in Fig. 5. The phase is parabolic, indicating nearly linear, positive chirp. There is a linear term in the phase associated with a frequency shift from the reference wavelength of the fit, which is not significant. Other deviations from a quadratic phase (linear chirp) are small.

pulse electric field. Fig. 10 shows these results. While the widths are similar, some discrepancies occur in the wings. These discrepancies probably reflect inadequacies of the

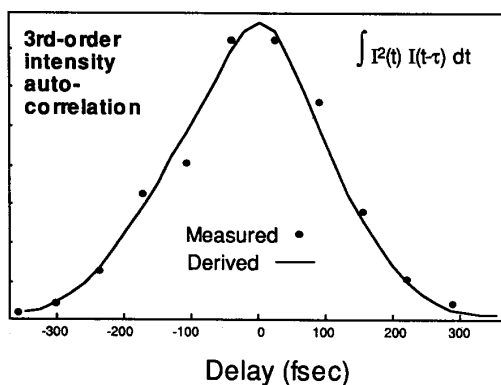


Fig. 9. The third-order intensity autocorrelation of the derived pulse and the measured pulse third-order intensity autocorrelation.

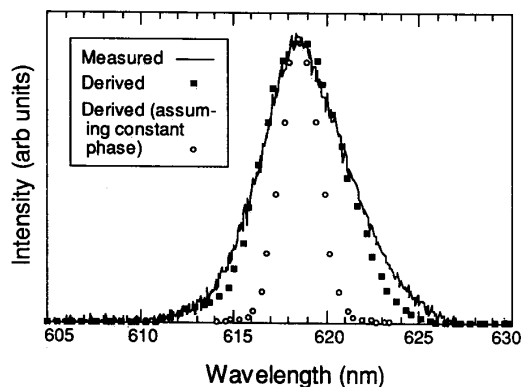


Fig. 10. Measured- and derived-pulse spectra. Also shown for comparison is a derived spectrum obtained by using the derived pulse intensity, but assuming constant phase, instead of the derived linear chirp. This latter spectrum is significantly narrower than the measured and derived spectra, illustrating the importance of the derived chirp.

assumed model and should be reduced when a more sophisticated algorithmic method is used to extract the pulse without assumptions regarding its intensity. For comparison, a spectrum is also shown in Fig. 10 that has been derived from the amplitude of the fit only and by assuming a constant phase. It is clear that the derived nonzero chirp has significantly broadened the spectrum of the derived pulse.

It should be mentioned that the measurable pulse parameters (energy, pulse length, spectrum) exhibited both shot-to-shot jitter and drift during the measurement, which required over twenty minutes. Consequently, the derived result is somewhat less meaningful than we would like—perhaps an unavoidable problem for a low-repetition-rate multishot measurement such as this. In a future publication [43] we will report single-shot FROG measurements that avoid these caveats.

We have also used fully compressed, transform-limited pulses and pulses with negative chirp, finding the expected behavior in all cases. Fig. 11 gives sample spectra obtained in these traces. In fact, the laser could be aligned

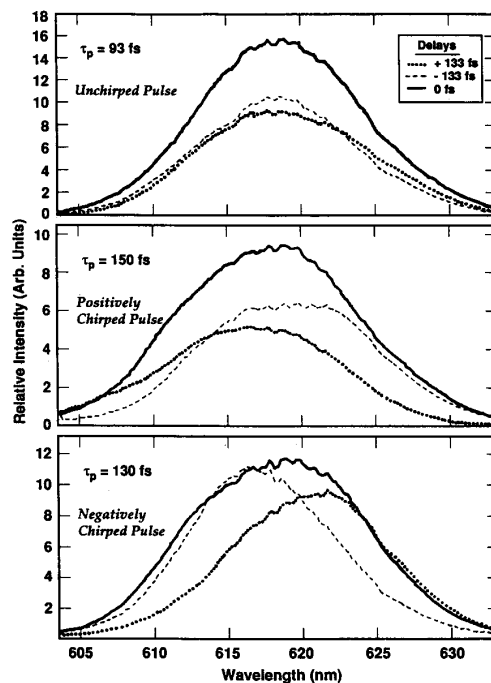


Fig. 11. Self-diffracted-pulse spectra for transform-limited, positively chirped, and negatively chirped pulses. For each pulse, spectra are shown for three different delays. The shifts in spectral content both illustrate the basis of FROG as a pulse diagnostic and demonstrate its use for rapid alignment of pulse compressors.

for the minimum pulsewidth easily by setting a nonzero delay and adjusting the pulse compressor until the mean wavelength of the spectrum of the self-diffracted light equalled that of scattered input-beam light. Indeed, it should be possible to build a simple autoaligning pulse compressor by comparing the FROG signal-pulse wavelengths for positive and negative delays.

We mentioned that it is possible to use a polarization-spectroscopy optical-gate arrangement. Such an arrangement simplifies the interpretation (see Appendix C). While results using a polarization-spectroscopy geometry will be discussed in more detail in the future [43], we should point out here that both geometries, self-diffraction and polarization spectroscopy, have advantages. Self-diffraction requires no optical components in the beams and thus should be best for extremely short pulses. Polarization spectroscopy, on the other hand, is perhaps easier to set up and allows a greater delay range in single-shot arrangements because a larger beam angle is possible.

In conclusion, we have developed and demonstrated a new technique for characterizing ultrashort pulses. This method involves obtaining simultaneous time- and frequency-resolved information regarding the pulse. It is experimentally quite simple and should be particularly effective for measuring UV pulses and for extension to single-shot operation. In addition, it should be a very convenient and intuitive method for displaying ultrashort pulses.

APPENDIX A

DERIVATION OF THE PULSE ELECTRIC FIELD FROM THE SIGNAL FIELD

It is straightforward to obtain the pulse electric field from the signal field $E_{\text{sig}}(t, \tau)$. The signal field is given by $E_{\text{sig}}(t, \tau) \propto [E(t)]^2 E^*(t - \tau)$, so we can compute the quantity:

$$\begin{aligned} \int_{-\infty}^{\infty} E_{\text{sig}}^*(t + \tau, \tau) d\tau &\propto \int_{-\infty}^{\infty} [E^*(t + \tau)]^2 E(t) d\tau \\ &\propto E(t) \left[\int_{-\infty}^{\infty} [E^*(t + \tau)]^2 d\tau \right] \propto E(t) \end{aligned} \quad (\text{A1})$$

where the bracketed quantity can be seen to be independent of t by a simple change of variables ($\tau \rightarrow t + \tau$).

APPENDIX B

AMBIGUITIES IN FROG MEASUREMENTS

It is important to give a more rigorous discussion of the ambiguities in FROG measurements. Phase retrieval is known to possess "trivial" ambiguities. If $E_{\text{sig}}(x, y)$ is the correct solution, then additional ambiguous solutions can also result [34]:

- 1) $E_{\text{sig}}(x, y) \exp(i\varphi_0)$, where φ_0 is a constant;
- 2) $E_{\text{sig}}(x - x_0, y - y_0)$, where x_0 and y_0 are constants; and
- 3) $E_{\text{sig}}^*(-x, -y)$.

Despite their name, it is important to verify that these ambiguities lead, in fact, only to trivial and insignificant ambiguities in the pulse field. The first two ambiguities yield, respectively, an arbitrary constant phase factor and an arbitrary shift in time to the pulse field, which are of no concern in ultrashort pulse measurement; that is, they are not physically significant. The third ambiguity above is inconsistent with (2) and thus does not occur in FROG.

Other ambiguities result only by chance, depending on the precise data, and are exceedingly unlikely [29], [31]–[33].

We should also mention that the spectrogram is known to have an additional ambiguity: the relative phase of well-separated pulses in a multiple-pulse field [26]. To see this, let $S_E(\omega, \tau)$ be the spectrogram of the function $E(t)$. If $E(t) = E_1(t) + E_2(t)$, in which these two component fields are well separated in time (i.e., by much more than the window duration), then $S_E(\omega, \tau) = S_{E_1}(\omega, \tau) + S_{E_2}(\omega, \tau)$ because the cross terms are zero. Since the spectrogram is a squared magnitude, the relative phase of the two fields is ambiguous. FROG, on the other hand, has cross terms that are not present in the spectrogram because, in FROG, the gate is essentially the pulse itself and is *always* as broad in time as the pulse to be measured. Thus, FROG avoids the only known physically significant ambiguity of the spectrogram.

Finally, we also should mention that use of second-harmonic generation (SHG) as the FROG nonlinearity provides an exception to these arguments. Use of SHG yields

an ambiguity in the direction of time. To see this, we write the SHG FROG signal as:

$$I_{\text{FROG}}^{\text{SHG}}(\omega, \tau) = \left| \int_{-\infty}^{\infty} E(t)E(t - \tau) \exp(-i\omega t) dt \right|^2 \quad (\text{B1})$$

Performing a simple change of variables $t' = t - \tau$ and dropping the primes, we find that:

$$I_{\text{FROG}}^{\text{SHG}}(\omega, \tau) = \left| \int_{-\infty}^{\infty} E(t)E(t + \tau) \exp(-i\omega t) dt \right|^2 \quad (\text{B2})$$

Thus, the SHG FROG signal is always symmetrical in the delay variable τ . As a result, among other ambiguities, it will not be possible to distinguish the direction of time for the pulse. Nevertheless, SHG FROG may have some applications, perhaps for low-intensity pulses.

APPENDIX C

THE INSTANTANEOUS FREQUENCY VERSUS TIME FOR SMOOTH PULSES

For not-too-pathological pulse shapes, it is possible to derive the approximate pulse instantaneous frequency directly from the FROG trace, without an iterative algorithm. Observe from Fig. 1 that the signal pulse will be centered at and have maximum strength at about the time $\tau/3$ (an exact result for Gaussian-intensity pulses). Because the expression for the signal frequency in self-diffraction is $\Omega = 2\omega_1 - \omega_2$, the instantaneous frequency of the signal pulse will be: $\Omega(\tau) \approx 2\omega(\tau/3) - \omega(-2\tau/3)$, where $\omega(t)$ is the instantaneous frequency of the pulse at time t . To obtain $\omega(t)$ in terms of $\Omega(\tau)$, we expand both functions in Taylor series, obtaining:

$$\omega(t) \approx \sum_{n=0}^{\infty} \frac{3^n t^n \Omega^{(n)}(0)}{n! [2 - (-2)^n]} \quad (\text{C1})$$

the first few terms of which are:

$$\begin{aligned} \omega(t) &\approx \Omega(0) + \frac{3}{4} \Omega'(0)t - \frac{9}{4} \Omega''(0)t^2 \\ &\quad + \frac{9}{20} \Omega'''(0)t^3 + \dots \end{aligned} \quad (\text{C2})$$

where $\Omega^{(n)}(0)$ is the n th derivative of $\Omega(\tau)$ evaluated at $\tau = 0$. For the simple case of linear chirp, if the FROG signal frequency is $\Omega(\tau) = \alpha\tau$, then $\omega(t) \approx 3/4 \alpha t$.

Use of a polarization-spectroscopy optical-gate arrangement yields a simpler result. The signal field will be given by $E_{\text{sig}}(t, \tau) \propto E(t) |E(t - \tau)|^2$, so the signal pulse will be centered at $2\tau/3$. The signal frequency will be $\Omega = \omega_1 - \omega_2 + \omega_2 = \omega_1$, so $\Omega(\tau) \approx \omega(2\tau/3)$. Thus, for polarization spectroscopy,

$$\omega(t) \approx \Omega(3t/2). \quad (\text{C3})$$

For the simple case of linear chirp, if the polarization-spectroscopy FROG signal frequency is $\Omega(\tau) = \alpha\tau$, then $\omega(t) \approx 3/2\alpha t$. Thus, while the polarization-spectroscopy result is simpler, self-diffraction FROG is more sensitive to chirp.

ACKNOWLEDGMENT

The authors would like to acknowledge the assistance of A. G. Kostenbauder.

REFERENCES

- [1] E. P. Ippen and C. V. Shank, *Ultrashort Light Pulses—Picosecond Techniques and Applications*, S. L. Shapiro, Ed. Berlin: Springer-Verlag, 1977, p. 83.
- [2] J. A. Giordmaine, P. M. Rentzepis, S. L. Shapiro, and K. W. Wecht, "Two-photon excitation of fluorescence by picosecond light pulses," *Appl. Phys. Lett.*, vol. 11, pp. 216–218, 1967.
- [3] N. G. Basov, V. É. Pozhar, and V. I. Pustovoit, "Measurement of the duration of high-power ultrashort optical pulses," *Sov. J. Quantum Electron.*, vol. 15, pp. 1429–1431, 1985.
- [4] J.-C. M. Diels, J. J. Fontaine, I. C. McMichael, and F. Simoni, "Control and measurement of ultrashort pulse shapes (in amplitude and phase) with femtosecond pulses," *Appl. Opt.*, vol. 24, pp. 1270–1282, 1985.
- [5] R. Trebino, C. C. Hayden, A. M. Johnson, W. M. Simpson, and A. M. Levine, "Chirp and self-phase modulation in induced-grating autocorrelation measurements of ultrashort pulses," *Opt. Lett.*, vol. 15, pp. 1079–1081, 1990.
- [6] J. T. Manassah, "Direct and second-harmonic interferometric determination of chirped pulse parameters," *Appl. Opt.*, vol. 26, pp. 2941–2942, 1987.
- [7] C. Yan and J. C. Diels, "Amplitude and phase recording of ultrashort pulses," *J. Opt. Soc. Amer. B*, vol. 8, pp. 1259–1263, 1991.
- [8] K. Naganuma, K. Mogi, and H. Yamada, "General method for ultrashort light pulse chirp measurement," *IEEE J. Quantum Electron.*, vol. 25, pp. 1225–1233, 1989.
- [9] T. Kobayashi, F.-C. Guo, A. Morimoto, T. Sueta, and Y. Cho, "Novel method of waveform evaluation of ultrashort optical pulses," in *Ultrafast Phenomena IV*, D. H. Auston and K. B. Eissenthal, Eds. Berlin: Springer-Verlag, 1984, pp. 93–95.
- [10] K. Naganuma, K. Mogi, and H. Yamada, "Time direction determination of asymmetric ultrashort optical pulses from second-harmonic generation autocorrelation signals," *Appl. Phys. Lett.*, vol. 54, pp. 1201–1202, 1989.
- [11] J. Jansky and G. Corradi, "Full intensity profile analysis of ultrashort laser pulses using four-wave mixing or third-harmonic generation," *Opt. Commun.*, vol. 60, pp. 251–256, 1986.
- [12] N. G. Paulter and A. K. Majumdar, "A new triple correlator design for the measurement of ultrashort pulses," *Opt. Commun.*, vol. 81, pp. 95–100, 1991.
- [13] A. S. L. Gomes, V. L. da Silva, and J. R. Taylor, "Direct measurement of nonlinear frequency chirp of Raman radiation in single-mode optical fibers using a spectral window method," *J. Opt. Soc. Amer. B*, vol. 5, pp. 373–379, 1988.
- [14] G. Szabo, A. Müller, and Z. Bor, "A sensitive single-shot method to determine duration and chirp of ultrashort pulses with a streak camera," *Opt. Commun.*, vol. 82, pp. 56–62, 1991.
- [15] J. E. Rothenberg and D. Grischkowsky, "Measurement of optical phase with subpicosecond resolution by time-domain interferometry," *Opt. Lett.*, vol. 12, pp. 99–101, 1987.
- [16] R. L. Fork, C. H. Brito-Cruz, P. C. Becker, and C. V. Shank, "Compression of optical pulses to six femtoseconds by using cubic phase compensation," *Opt. Lett.*, vol. 12, pp. 483–485, 1987.
- [17] R. L. Fork, C. V. Shank, C. Hirlimann, R. Yen, and W. J. Tomlinson, "Femtosecond white-light continuum," *Opt. Lett.*, vol. 8, pp. 1–3, 1983.
- [18] T. F. Albrecht, K. Seibert, and H. Kurz, "Chirp measurement of large-bandwidth femtosecond optical pulses using two-photon absorption," *Opt. Commun.*, vol. 84, pp. 223–227, 1991.
- [19] F. Reynaud, F. Salin, and A. Barthelemy, "Measurement of phase shifts introduced by nonlinear optical phenomena on subpicosecond pulses," *Opt. Lett.*, vol. 14, pp. 275–277, 1989.
- [20] K. W. DeLong and J. Yumoto, "Chirped light and its characterization using the cross-correlation technique," *J. Opt. Soc. Amer. B.*, to be published.
- [21] J. L. A. Chilla and O. E. Martinez, "Direct determination of the amplitude and the phase of femtosecond light pulses," *Opt. Lett.*, vol. 16, pp. 39–41, 1991.
- [22] —, "Frequency-domain phase measurement of ultrashort light pulses. Effect of noise," *Opt. Commun.*, vol. 89, pp. 434–440, 1992.
- [23] —, "Analysis of a method of phase measurement of ultrashort pulses in the frequency domain," *IEEE J. Quantum Electron.*, vol. 27, pp. 1228–1235, 1991.
- [24] M. Beck and I. A. Walmsley, "Experimental characterization of the intensity and phase of asymmetric 60-fs pulses from a CPM dye laser," presented at Optical Society of America Annual Meeting, 1991, post-deadline paper.
- [25] W. Koenig, H. K. Dunn, and L. Y. Lacy, "The sound spectrograph," *J. Acoust. Soc. Amer.*, vol. 18, pp. 19–49, 1946.
- [26] S. H. Nawab, T. F. Quatieri, and J. S. Lim, "Signal reconstruction from short-time Fourier transform magnitude," *IEEE Trans. Acoustics, Speech, Sig. Process.*, vol. ASSP-31, pp. 986–998, 1983.
- [27] R. A. Altes, "Detection, estimation, and classification with spectrograms," *J. Acoust. Soc. Am.*, vol. 67, pp. 1232–1246, 1980.
- [28] L. Cohen, "Time-frequency distributions—A review," *Proc. IEEE*, vol. 77, pp. 941–981, 1989.
- [29] H. Stark, *Image Recovery: Theory and Application*. Orlando, FL: Academic, 1987.
- [30] R. P. Millane, "Phase retrieval in crystallography and optics," *J. Opt. Soc. Amer. A.*, vol. 7, pp. 394–411, 1990.
- [31] R. Barakat and G. Newsam, "Necessary conditions for a unique solution to two-dimensional phase recovery," *J. Math. Phys.*, vol. 25, pp. 3190–3193, 1984.
- [32] R. G. Lane, W. R. Fright, and R. H. T. Bates, "Direct phase retrieval," *IEEE Trans. Acoust. Speech Signal Process.*, vol. ASSP-35, pp. 520–525, 1987.
- [33] D. Israelevitz and J. S. Lim, "A new direct algorithm for image reconstruction from Fourier transform magnitude," *IEEE Trans. Acoust. Speech Signal Process.*, vol. ASSP-35, pp. 511–519, 1987.
- [34] J. R. Fienup, "Reconstruction of a complex-valued object from the modulus of its Fourier transform using a support constraint," *J. Opt. Soc. Amer. A*, vol. 4, pp. 118–123, 1987.
- [35] J. H. Seldin and J. R. Fienup, "Iterative blind deconvolution algorithm applied to phase retrieval," *J. Opt. Soc. Amer. A*, vol. 7, pp. 428–433, 1990.
- [36] J. R. Fienup, "Phase retrieval algorithms: A comparison," *Appl. Opt.*, vol. 21, pp. 2758–2769, 1982.
- [37] R. G. Lane, "Phase retrieval using conjugate gradient minimization," *J. Mod. Opt.*, vol. 38, pp. 1797–1813, 1991.
- [38] C. E. Heil and D. F. Walnut, "Continuous and discrete wavelet transforms," *SIAM Rev.*, vol. 31, pp. 628–666, 1989.
- [39] While the spectrogram is very useful, it is not considered to be the ideal time- and frequency-resolved quantity. The Wigner distribution and wavelet transform, for example, are much more popular at the moment. In the authors' opinions, however, it is the spectrogram, or, more precisely, the FROG trace, that is the most easily experimentally measured time- and frequency-resolved quantity for ultrashort pulses. The above mentioned alternative measures require such quantities as a time-reversed replica of the pulse or a variable-frequency and simultaneously variable-length window. Such quantities are quite difficult to obtain optically. On the other hand, the spectrogram's main inadequacy is that its fixed-length window cannot simultaneously provide good resolution of both long- and short-term variations. This is not a problem in ultrashort-pulse measurement, where the dynamic range of variations is typically much smaller than that in acoustics problems, for example. It may also be the case that, because in FROG the gate has exactly those time scales as the pulse, FROG may actually avoid the above problem in general, but we have not investigated this issue as yet.
- [40] H. L. Fragnito, J.-Y. Bigot, P. C. Becker, and C. V. Shank, "Evolution of the vibronic absorption spectrum in a molecule following impulsive excitation with a six fs optical pulse," *Chem. Phys. Lett.*, vol. 160, pp. 101–104, 1989.
- [41] J. H. Glowina, J. A. Misewich, and P. P. Sorokin, "Femtosecond transition-state absorption spectroscopy of Bi atoms produced by photodissociation of gaseous Bi₂ molecules," *J. Chem. Phys.*, vol. 92, pp. 3335–3347, 1990.
- [42] A. Freiberg and P. Saari, "Picosecond spectrochronography," *IEEE J. Quantum Electron.*, vol. QE-19, pp. 622–630, 1983.
- [43] D. J. Kane and R. Trebino, "Single-shot measurement of the intensity and phase of a femtosecond pulse," *Ultrafast Phenomena IX*, 1992, in press.



Daniel J. Kane was born in Wilmington, DE, in 1960. In 1983, he received the B.S. degree in physics from Montana State University, Bozeman, MT. He received the M.S. and Ph.D. degrees in physics from the University of Illinois, Urbana-Champaign, in 1985 and 1989, respectively.

In 1989, he started a post-Doctoral Fellow in Group CLS-4 at Los Alamos National Laboratories studying nonlinear optics and ultrafast lasers.

In 1992, he joined Southwest Sciences, Inc. His current interests are nonlinear optics, ultrafast pulse measurement, and diode laser spectroscopy.

Dr. Kane is a member of the American Physical Society, the Optical Society of America, and Sigma Xi.



Rick Trebino was born in Boston, MA, on January 18, 1954. He received the B.A. degree in physics from Harvard University, Cambridge, MA, in 1977 and the M.S. and Ph.D. degrees in applied physics from Stanford University, Stanford, CA, in 1979 and 1983, respectively. His dissertation research involved the development of frequency-domain methods for the measurement of ultrafast phenomena.

He worked as a Physical Sciences Research Associate at Stanford University from 1983 to 1986 and then joined Sandia National Labs, where he is currently employed. His current research mainly involves the development of novel techniques and technology for the study of ultrafast phenomena. He has also studied, both theoretically and experimentally, higher-order wave-mixing effects. Finally, he has developed a novel immunoassay for measuring trace constituents of blood, as well as other media, such as milk.

Dr. Trebino is a member of the American Association for the Advancement of Science, the American Physical Society, and the Optical Society of America.